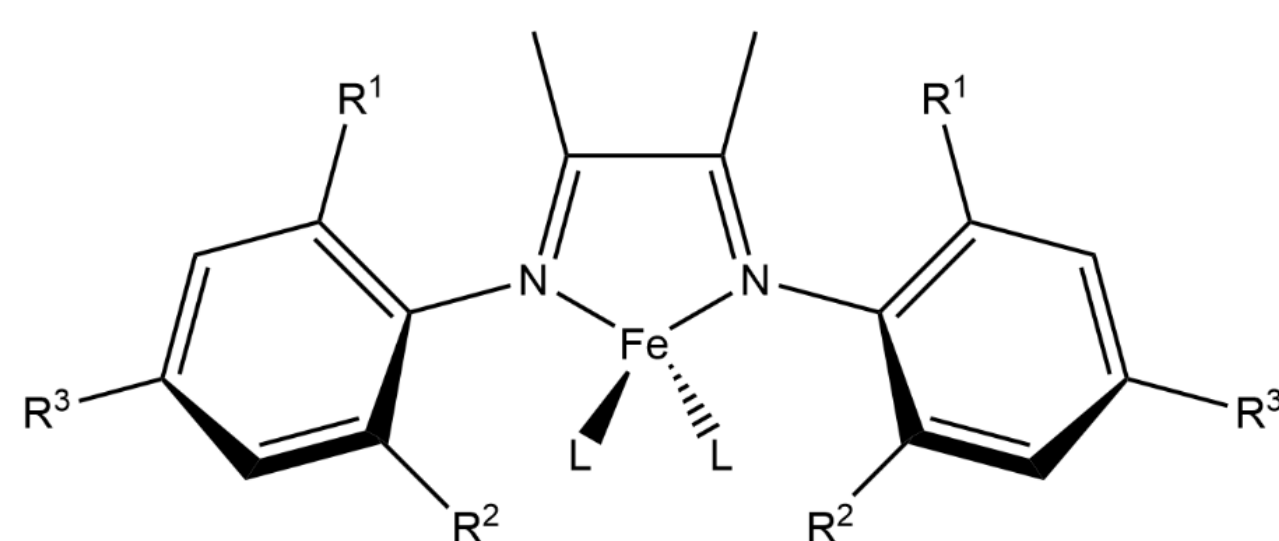


Abstract

Iron dibromide complexes bearing bidentate α -diimine (DI) ligands $^ArN=C(Me)-(Me)C=N^{Ar}$ (Ar = dpp and Mes; dpp = 2,6-diisopropylphenyl; Mes = 2,4,6-trimethylphenyl), upon reduction, have been shown to promote catalytic hydrosilylation of 1-hexene with phenylsilane in a range of good to excellent yields. To better understand the factors responsible for the variation in yields, proposed ArDI iron catalysts bound by cyclooctadiene (COD) have been explored computationally for electronic structure analysis. The electronic structure of proposed iron-COD hydrosilylation catalysts was studied using computational analysis to predict properties of the catalysts before they will be synthesized experimentally. Density Functional theory (DFT) calculations were performed at the B3LYP level of theory on a series of proposed iron-COD catalysts. Geometry optimization, Mossbauer parameters, and numerical frequency computations have been performed, and computed values were compared to experimental data where possible. Computational analysis has been performed for $dppDIFe(COD)$ and isomers of $^{2iPr}DIFe(COD)$. These catalysts are predicted to have high spin iron(I) centers antiferromagnetically coupled to a redox-active, monoreduced DI ligands as the lowest energy electronic structure outcome. These predictions will be used in ongoing projects to identify the optimal Mossbauer isomer shift ranges to produce high yield reactions.

Background

Metal	Price/gram (99.99% pure) ¹	% of Earth's crust ²	Allowed Oral Exposure ³ (ug/day)
Platinum	\$290	0.0000037%	100
Iron	\$6.06	6.3%	13000



L= COD or Toluene

A: $R^1, R^2 = i\text{-Pr}$; $R^3 = H$
B-E: $R^1 = i\text{-Pr}$; $R^2, R^3 = H$
F: $R^1, R^2, R^3 = Me$
G: $R^1, R^2 = Et$; $R^3 = H$
H: $R^1 = t\text{-Bu}$; $R^2, R^3 = H$
J: $R^1, R^2 = H$; $R^3 = t\text{-Bu}$

- Using catalysts and employing less toxic and more abundant compounds are key principles in green chemistry.⁴
- Iron has unpaired electrons and is paramagnetic, which allows for electron transfer to form radical ligands, or "redox-active" ligands.

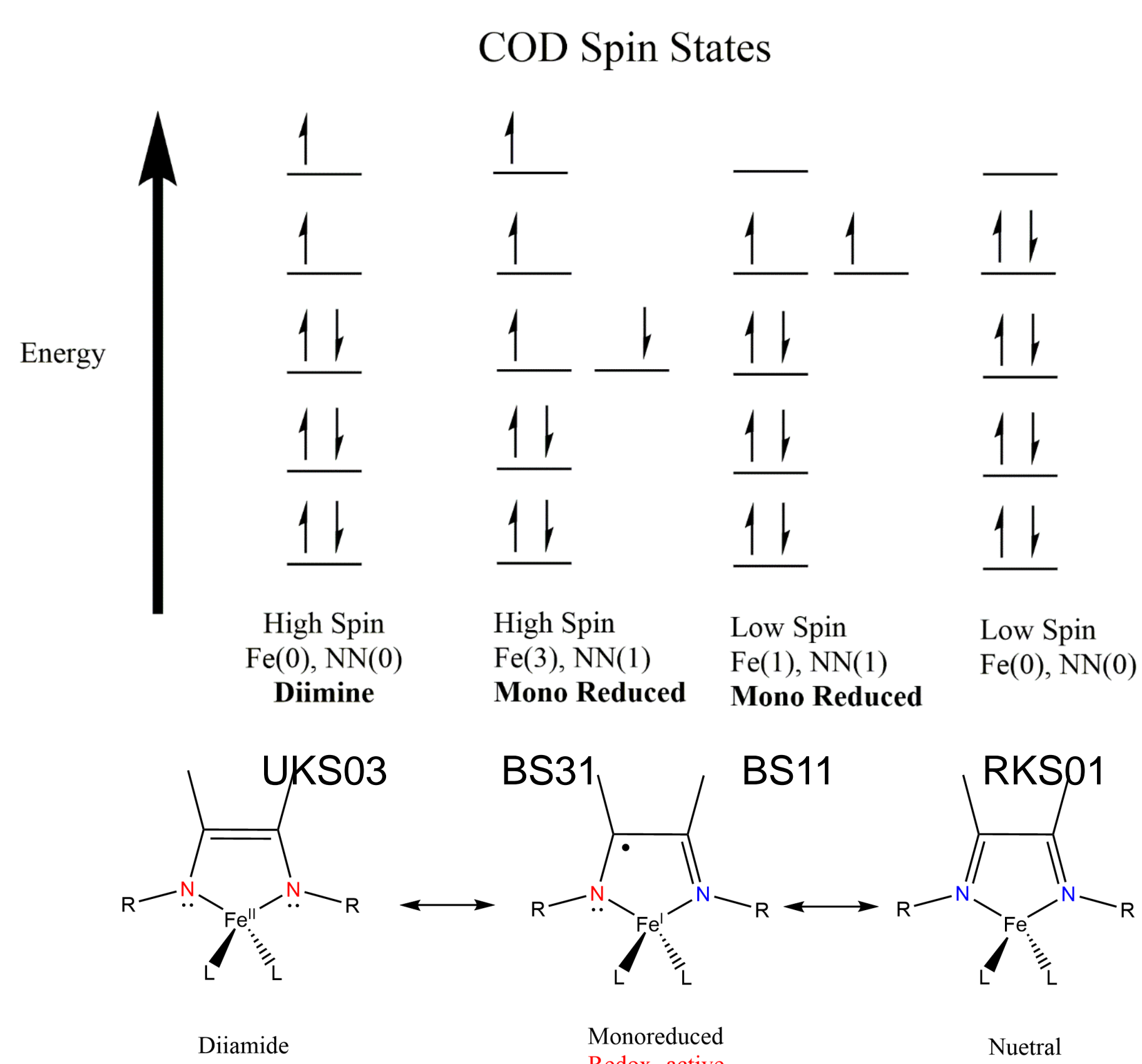
- Ligands used in this study can aid in delocalizing the electrons, stabilizing the catalyst and minimizing radical formations in the organic species.⁵
- This study included computations on multiple iron cyclooctadiene (COD) complexes bound by alpha diimine (DI) ligands through multiple computations.

- ArDIFeBr_2 precatalysts were found in previous experimental studies to provide a range of hydrosilylation yields. Understanding the active catalyst will be necessary to explain the observed yields.⁶

- Electronic models of the ArDIFeCOD active catalysts will be explored.

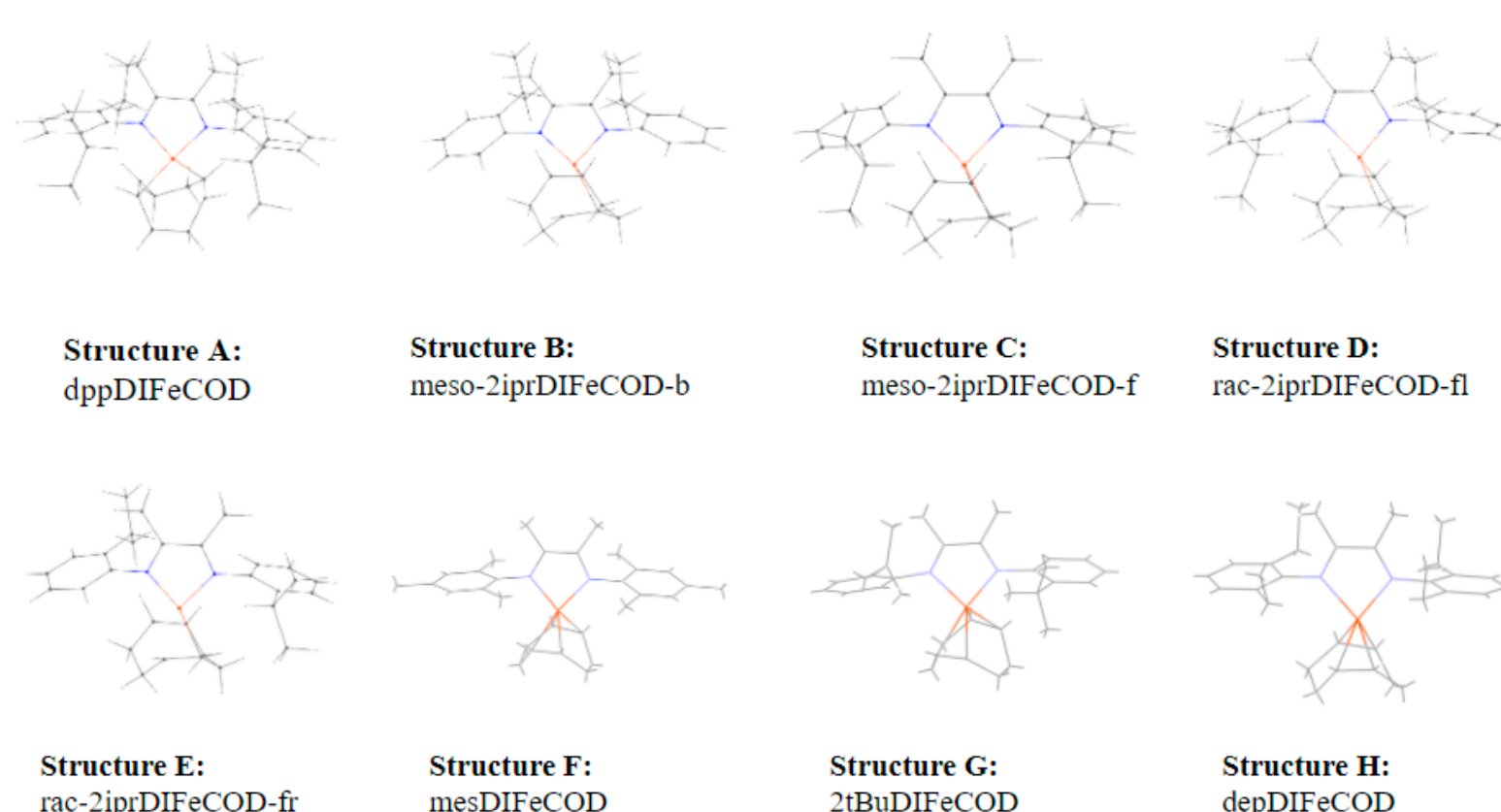
Electronic Structures

- $dppDIFeCOD$ active catalyst compound was shown to be in the monoreduced resonance form in the literature.⁷⁻⁸
- Mossbauer data also showed the high spin state for the iron center.⁷
- The precatalysts had the neutral ligand form and the active catalyst had a ligand in the monoreduced form, showing that this ligand was behaving in a redox-active fashion.⁶
- Redox-active behavior allows for the transfer of an unpaired electron from the iron center to the ligand which allows for hydrosilylation to be selectively favored.
- The goal of this project is to reproduce the data for $dppDIFeCOD$ and expand data for other smaller steric substituents in the series.



Computational Methods

- All DFT calculations were performed in the gas phase with the ORCA program package.⁹
- The geometry optimizations of the complexes and single-point energy calculations on the optimized geometries were carried out at the B3LYP level of DFT.⁹⁻¹¹
- Triple- ζ quality basis sets def2-TZVP with one set of polarization functions on the metals and on the atoms directly coordinated to the metal center were used. For the carbon and hydrogen atoms, slightly smaller polarized split-valence def2-SV(P) basis sets were used.¹²⁻¹⁴
- Numerical frequencies were calculated at the same level of theory to confirm that a global energy minimum had been achieved and that there were no imaginary frequencies for BS31 of $dppDIFeCOD$ (**A**), $^{2iPr}DIFeCOD$ (**B-E**), $mesDIFeCOD$ (**F**), and $^{2tBu}DIFeCOD$ (**G**).
- Non-relativistic single-point calculations on the optimized geometry were carried out to predict Mössbauer spectral parameters (i.e. isomer shifts and quadrupole splittings).



$^{2iPr}DIFeCOD$ (**B-E**): *racemic* (**D/E**) and *meso* (**B/C**) isomers were explored with different input conformations for geometry optimization to determine if each would converge to the same outputs

Computational Results

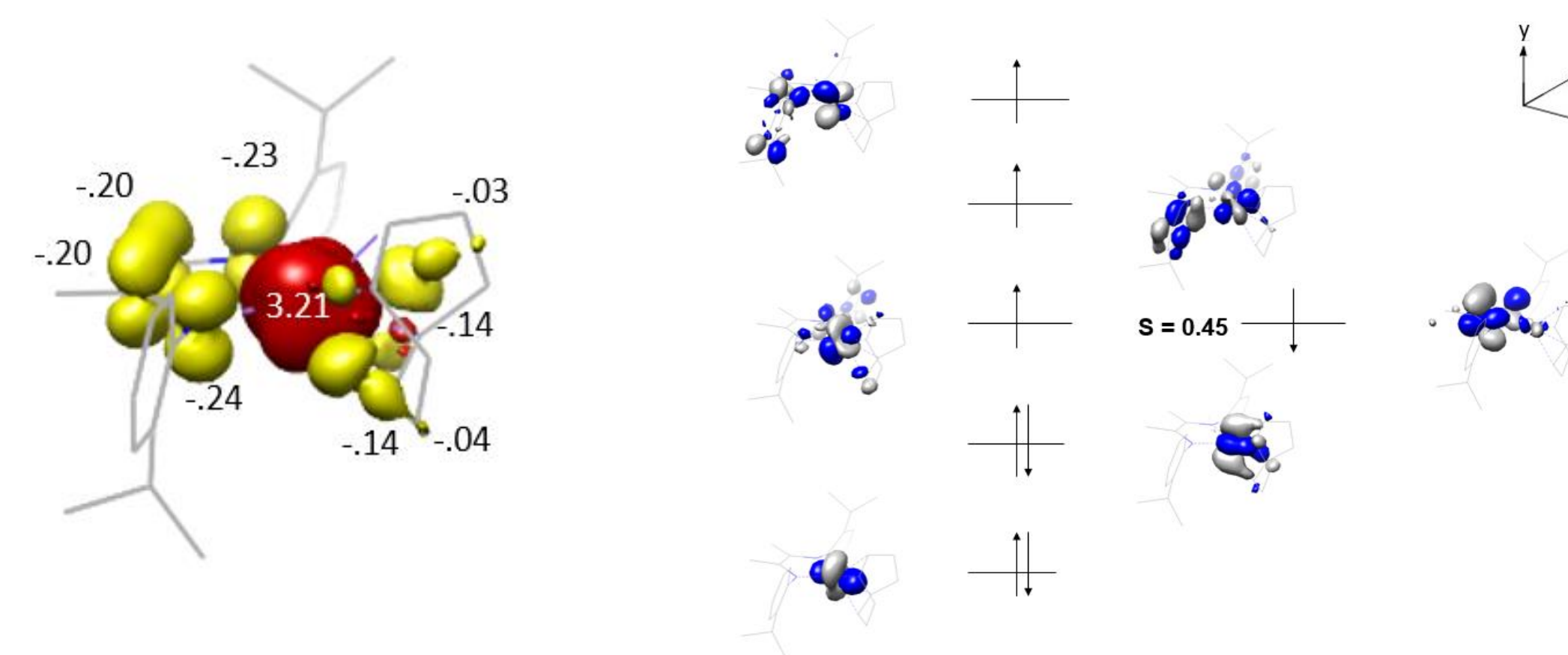
Comparative values for structures A-E

- For each of the structures & each electronic structure model, geometry optimization, numerical frequency, and Mossbauer computations were performed.
- For the lowest energy electronic structure model of BS31 for each complex, a spin density plot and a qualitative molecular orbital picture was created; *rac-^{2iPr}DIFeCOD-fr* (**E**) will be used as an example.
- For $^{2iPr}DIFeCOD$, both *racemic* conformations, *rac-fr* (**E**) and *rac-fl* (**D**), had the lowest Final Single Point Energies and were energetically similar, but *rac-fr* (**E**) was the global minimum, so only **E** is included.

Catalyst	Model	FSPE (kcal/mol)	Global or local minimum	Computed IS (mm/s)	Experiment al IS (mm/s)	Computed QS (mm/s)	Experimental QS (mm/s)
A	BS31	-1741002	global	0.39	0.48	1.554	1.30(1)
E	BS31	-1593205	global	0.47	n/a	1.249	n/a
F	BS31	-1593216	global	0.579	0.46	1.397	0.98
G	BS31	-1593216	global	0.672	n/a	1.657	n/a
H	BS31	-1642474	TBD	TBD	n/a	TBD	n/a

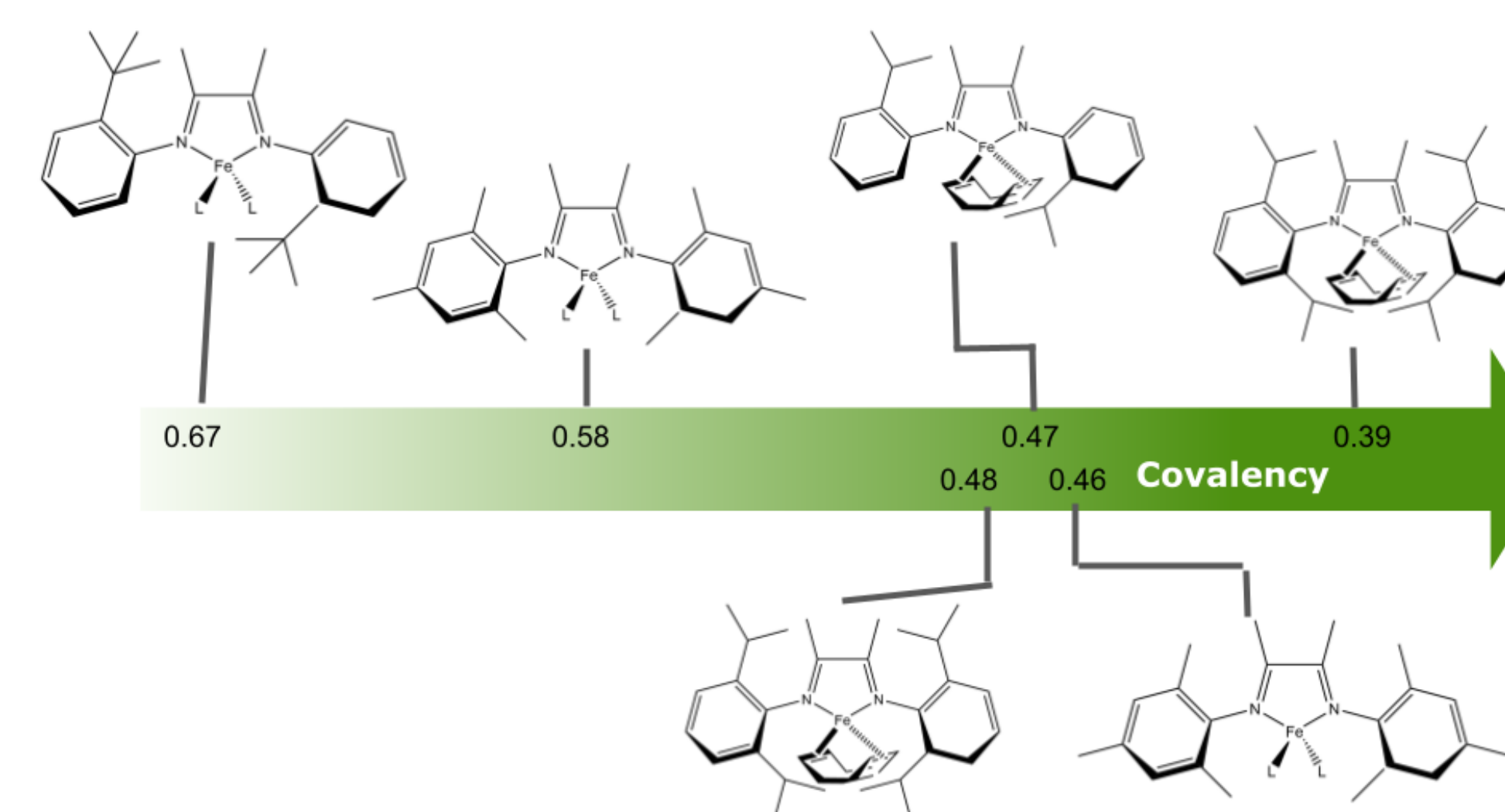
rac-^{2iPr}DIFeCOD-fr (**E**) Spin Density plot (left) and Qualitative Molecular Orbital diagram (right) for BS31 model

- The Spin density plot shows overall unpaired electrons as 1.99 consistent with the expected number of 2 unpaired electrons on Iron.
- The qualitative molecular orbital diagram shows antiferromagnetic coupling which indicates a reasonable overlap of 0.45 which is expected in the BS31 model.



Mossbauer trend arrow

- Computational data from this project is shown on the top for $^{2tBu}DIFeCOD$ (**G**), $mesDIFeCOD$ (**F**), *rac-^{2iPr}DIFeCOD-fr* (**E**), and $dppDIFeCOD$ (**A**) respectively.
- Literature experimental data is shown for the comparisons found on the bottom of the arrow.⁷
- The predicted Mossbauer isomer shift from computational work is within tolerance¹⁵ for the experimental isomer shift and quadrupole splitting for $dppDIFeCOD$ and $mesDIFeCOD$ was within tolerance for the quadrupole splitting and only 0.02 outside of tolerance for the isomer shift⁷



Conclusions

- For all structures studied, the BS31 energy model was the lowest energy model.
- High spin Fe(I) antiferromagnetically coupled to the monoreduced DI resonance form (denoted as BS31) is the lowest energy electronic structure description.
- The reproducibility of the $dppDIFeCOD$ and $mesDIFeCOD$ Mossbauer literature data furthers confidence in the computational data predicted for unknown compounds such as $^{2iPr}DIFeCOD$ that have yet to be isolated experimentally.
- The computed $^{2iPr}DIFeCOD$ catalyst is predicted to have a similar isomer shift to the experimental $mesDIFeCOD$ and $dppDIFeCOD$ isomer shifts.
- The computed $^{2iPr}DIFeCOD$ catalyst is predicted to have a less covalent isomer shift than the computed $dppDIFeCOD$ isomer shift, which will be interesting to study in the lab for impact on catalysis.

Future Work

- Continue to add computational and experimental Mossbauer shifts to the Mossbauer arrow for more compounds with new ligands.
- Run numerical frequency computations for **H** to see if it is a global minimum.
- Compare computational Mossbauer trend arrow with reactivity in the lab to predict an optimal Mossbauer range for highly reactive catalysts in the series.
- Synthesize studied active catalysts in the lab, specifically $^{2iPr}DIFeCOD$ to compare experimental Mossbauer data and reactivity with computations.

References

- ¹<http://SigmaAldrich.com> (accessed Oct 28, 2020)
- ²Abundance in Earth's Crust of the Elements <http://periodictable.com> (accessed Oct 28, 2020)
- ³Guideline on the Specification Limits for Residues of Metal Catalysts set by the European Medicines Agency www.ema.europa.eu (accessed Oct 28, 2020)
- ⁴12 Principles of Green Chemistry <http://acs.org> (accessed Oct 28, 2020)
- ⁵Cody, C. Schulz, E. Hoyt, H. Poster, INOR-229, 255th National Meeting of the American Chemical Society, New Orleans, LA, March 18-22, 2018.
- ⁶Supej, J. Volkov A. Darkoa, L. West, A. Darmon, M. Schulz, E. Wheeler, A. Hoyt, H. *Polyhedron* **2016**, *114*, 403-414.
- ⁷Schmidt, A., Kennedy, R., Bezdek, J. Chirik, J. *J. Am. Chem. Soc.* **2018**, *140* (9), 3443-3453.
- ⁸Lee, H.; Campbell, M. G.; Sánchez, R.; Börgel, J.; Raynaud, J.; Parker, S.E.; Ritter, T. *Organometallics* **2016**, *35*, 2923-2929.
- ⁹Lee, C. Yang, W. Parr, R. *Rev. B* **1988**, *37*, 785.
- ¹⁰Becke, A. *J. Chem. Phys.* **1986**, *84*, 4524.
- ¹¹Becke, A. *J. Chem. Phys.* **1993**, *98*, 5648.
- ¹²Eichkorn, K., Weigend, F., Treutler, O., Ahlrichs, R., *Theor. Chem. Acc.* **1997**, *97*, 119.
- ¹³Eichkorn, K., Treutler, O., Ohm, H., Haser, M., Ahlrichs, R., *Chem. Phys. Lett.* **1995**, *240*, 283.
- ¹⁴Eichkorn, K., Treutler, O., Ohm, H., Haser, M., Ahlrichs, R., *Chem. Phys. Lett.* **1995**, *242*, 652.
- ¹⁵Rörmelt, R.; Ye, S.; Neese, F. *Inorg. Chem.* **2009**, *48*, 784.

Acknowledgments

- Knox College Paul K. Richter and Evelyn E. Cook Richter Memorial Trusts
- Glenn M. Nagel Undergraduate Research Fund Award in Chemistry and Biochemistry
- Hoyt Research Group & Knox Chemistry Department